Promising substitute of inconsistent algal alginates: exploring the biocompatible properties of di-O-acetylated, poly-L-guluronate-deficient alginate from soil bacterium *Pseudomonas aeruginosa* CMG1418

MUHAMMADI [1,*], SHABINA SHAFIQ [1], ZARRIN F. RIZVI [2]

[1] Centre for Bioresource Research, Islamabad, Pakistan

[2] Department of Botany, Government College Women University, Sialkot, Pakistan

Abstract

The structural inconsistencies in commercial algal alginates have limited their reliability and quality for various applications. Therefore, the biosynthesis of structurally consistent alginates is crucial to replace the algal alginates. Thus, this study aimed to investigate the structural and alginate's structural and functional properties of *Pseudomonas aeruginosa* CMG1418 as a substitute. To achieve this, the CMG1418 alginates were physiochemically characterized using various techniques such as transmission electron microscopy, Fourier-transform infrared ^{1}H-NMR, ^{13}C-NMR, and gel permeation chromatography. The synthesized CMG1418 alginate was then subjected to standard tests to evaluate its biocompatibility, emulsification, hydrophilic, flocculation, gelling, and rheological properties. The analytical studies revealed that CMG1418 alginate is an extracellular and polydisperse polymer with a molecular weight range of 20 000–250 000 Da. It comprises 76% poly-(1–4)-β-D-mannuronic acid (M-blocks), no poly-α-L-guluronate (G-blocks), 12% alternating sequences of β-D-mannuronic acid and α-L-guluronic acid (poly-MG/GM-blocks), 12% MGM-blocks, 172 degrees of polymerization, and di-O-acetylation of M-residues. Interestingly, CMG1418 alginate did not show any cytotoxic or antimetabolic activity. Moreover, compared to algal alginates, CMG1418 alginate exhibited higher and more stable flocculation efficiencies (70–90%) and viscosities (4500–4760 cP) over a wide range of pH and temperatures. Additionally, it displayed soft to flexible gelling abilities and higher water-holding capacities (375%). It also showed thermodynamically more stable emulsifying activities (99–100%) that surpassed the algal alginates and commercial emulsifying agents. However, only divalent and multivalent cations could slightly increase viscosity, gelling, and flocculation. In conclusion, this study explored a structurally di-O-acetylated and poly-G-blocks-deficient, biocompatible alginate, and its pH and thermostable functional properties. This research suggests that CMG1418 alginate is a superior and more reliable substitute for algal alginates in various applications, such as viscosifying, soft gelling, flocculating, emulsifying, and water-holding.

Key words: di-O-acetylated alginate, biocompatiblity, water-holding, emulsifying, flocculating, viscosifying

Introduction

Alginate, the second-largest polymer with growing industrial interest, is an unbranched and linear acidic polysaccharide composed of 1-4-linked β-D-mannuronic acid (M) and its C-5 epimer α-L-guluronic acid (G). It is extracted from marine brown algae and synthesized extra-cellularly by Gram-negative bacteria belonging to rRNA homology group I *Pseudomonas*, *Azotobacter*, and *Azomonas* (Bai et al., 2017; Zhang and Cheng, 2021). Alginates have a long history of use in various food and non-food industries, including emulsification, flocculation, thickening, water retention, gelling, texturizing, and sta-

* Corresponding author: Centre for Bioresource Research, Islamabad, Pakistan; email: muhammadi12@yahoo.com

bilization as gelling agents, thickeners, stabilizers, excipients, and drug carriers (Goh et al., 2012; Bai et al., 2017). Due to its multifunctional properties and extensive applications, there has been a rising interest in the development of alginates around the world (Bai et al., 2017). Currently, commercially available alginates are obtained from algal sources (Abraham et al., 2018; Valentine et al., 2020), but bacterial alginates remain untapped for industrial applications. The physical and functional properties of alginates mainly depend on several structural and molecular characteristics, including the monomer chemical composition and block structure, relative abundance and distribution of monomers, degree of acetylation, degree of polymerization (DP_n), and molecular weight (Mol. wt) (Fertah et al., 2017; Urtuvia et al., 2017).

The chemical structure of algal alginates (O-acetylation = 0) differs significantly from bacterial alginates, which have a well-defined chemical structure, high DP_n (Mol. wt), and O-acetyl groups exclusively on M-residues at O-2 and/or O-3 in varying degrees (Usov, 1999; Marinho-Soriano et al., 2006; Meena et al., 2020). Additionally, bacterial alginate has a different composition, M/G ratio, and block structure compared to algal alginate (Urtuvia et al., 2017).

The composition of algal alginates varies depending on various factors such as species (Fertah et al., 2017), specific parts of the same species, different breeding environments, changes in ocean temperature (Abraham et al., 2018; Valentine et al., 2020), harvest seasons, harvest locations, environmental pollution, processing methods, and others (Marinho-Soriano et al., 2006; Arunkumar, 2017). Algal alginates vary in composition, Mol. wt, and degree of physicochemical heterogeneity due to differences in species, harvest location, environmental factors, processing methods, and more (Windhues and Borchard, 2003; Fertah et al., 2017). As a result, it is challenging to maintain consistent quality and meet the demand for reliable alginate for industrial applications (Fertah et al., 2017). Consequently, there is an increasing demand for more reliable, structurally consistent, and superior-quality alginate sources that can be customized as alternatives to seaweed for alginate supply. For this purpose, bacterial fermentation has been investigated as an alternative production method explored to synthesize physiochemically consistent alginate (Remminghorst and Rehm, 2006).

Unlike algal alginates, bacterial alginates can be easily produced and tailored to obtain reproducible physicochemical characteristics and compositions, primarily in terms of Mol. wt and M/G distribution, by manipulating culture conditions during fermentation (Flores et al., 2015; Urtuvia et al., 2017). Bacterial alginates have the potential for commercial use in various industrial applications, as they are nontoxic and have been approved by the World Health Organization for therapeutic purposes and human consumption (MacDowell, 1974). However, the yield of alginate from *Azotobacter* is low due to stringent growth conditions, and genetic manipulation tools for *Azotobacter* have not yet been optimized (Bai et al., 2017). In contrast, the regulation of alginate biosynthesis in *Pseudomonas aeruginosa* has been extensively studied, and genetic manipulation tools for *Pseudomonas* are available, thereby enhancing alginate yield (Franklin et al., 2011; Muhammadi and Shafiq, 2019; Valentine et al., 2020). Furthermore, *P. aeruginosa* synthesizes alginate with a higher yield, an abundance of MM-blocks, a high M/G ratio, and Mol. Wt, making it a potential substitute for algal alginates (Windhues and Borchard, 2003). Despite its unique structural characteristics, biocompatibility, enhanced yield, and known genetic mechanism of biosynthesis, the functional properties of alginate from *P. aeruginosa* have not been studied for its place in the industry as an alternative to algal alginates. Therefore, the present study aimed to investigate the structural characteristics, *in vitro* biocompatibility, and functional properties of poly-G-deficient di-O-acetylated alginate from the indigenous soil bacterium *P. aeruginosa* CMG1418 to identify a structurally consistent alternative to algal alginates.

Materials and methods

Bacterial strain and culture medium

The Gram-negative bacterial strain CMG1418 utilized in this study was previously isolated from contaminated soil at the Jam Processing Unit of Ahmed Foods in Karachi and was found to produce an extracellular acidic polysaccharide (Muhammadi and Ahmed, 2006). The identification of bacterial strain CMG1418 was performed through 16S rRNA gene sequence homology searches as described previously (Muhammadi and Shafiq, 2019), using oligonucleotide primers (forward: 5′–CCCGGGA ACGTATTACCG–3′; reverse: 5′–GCYTAAYATGCAAG

TCGA-3′). The amplified PCR product was purified using the QIA quick PCR purification Kit (50) (QIAGEN, Germany), and the purified DNA was lyophilized at −50°C. The size and quantity of the polymerase chain reaction product were estimated relatively by horizontal agarose gel electrophoresis with 1 Kb DNA Ladder (Gene Craft) run parallel. The 16S rDNA was sequenced by Dideoxy chain-termination with ABI 3730 DNA Analyzer (Applied Biosystems, Cheshire, UK) as described earlier (Muhammadi and Shafiq, 2019) and submitted to GenBank (accession number: EF210102).

A minimal medium with a pH of 7 and containing sucrose (2%) as the sole carbon source was used to synthesize alginate, following the protocol previously described (Muhammadi and Shafiq, 2019). The bacterial strain CMG1418 was cultured in 1.3% nutrient broth (Sigma-Aldrich) at 30°C until it reached the log phase (OD600 ~0.75). Next, 5 ml of the culture was transferred to 500 ml Schott Duran (GL 45) graduated bottles (Germany), containing 400 ml of minimal medium. The culture was then grown statically in a microbiological incubator (Thermo Fisher Scientific) at 30°C for 12, 18, 24, 48, 72, 120, 150, 170, 300, and 360 h.

Dry cell mass determination

Bacterial cells from each culture with the designated incubation period underwent sedimentation through centrifugation at 12 000 rotations/min for 15 min. The resulting pellet was resuspended in NaCl (0.89%) and washed thrice until non-mucoid cells were obtained. The cell pellets were then dried in a Wheaton dry seal desiccator containing $CaCl_2$, and subsequently subjected to heat drying at 105°C in an electric oven (OSK 93MD145, Ogawa Seiki Co, Japan) until a consistent weight was attained, which was recorded as cell dry mass (CDM) (g/l).

Transmission electron microscopy (TEM) of alginate biosynthesis

TEM was utilized to examine the cellular synthesis of alginate and its concentration gradient around the cells, using the method described by Sabra et al. (2000). *P. aeruginosa* CMG1421 was grown statically in the aforementioned minimal medium for 12, 24, 48, 72, and 120 h at 30°C. Ruthenium red (RR) (0.5% w/v) was added to the cells in the growth medium and incubated at 27°C for 30 min. To fix the cells, glutardialdehyde (25% v/v) was added to a final concentration of 1.25% (v/v) and

incubated for 72 h at 27°C, followed by fixation at 4°C. The cells were collected through centrifugation at 4°C, resuspended in 0.1 M cacodylate buffer (pH 7.2), and washed thrice for 10 min at 27°C. The washed cells were immobilized in 2% (w/v) agar buffered with cacodylate (0.1 M, pH 7.2) and fixed with OsO_4 (1% w/v)-cacodylate (0.1 M, pH 7.2) overnight at 4°C. After dehydration on ice with acetone (25, 50, 75, 90, and 100%), the cells were finally embedded in epoxy resin. Ultrathin sections (40 nm) of the embedded CMG1418 alginate specimen were sliced using a diamond knife-fitted ultramicrotome (LKB 2088, Bromma, Sweden), collected on collodion grids (200 mesh, Cu), and blotted with Whatman paper 6. The CMG1418 alginate specimen was positively stained with a freshly prepared solution of RR (1.5%) for 2 min, followed by negative staining with uranyl acetate (1%) for 12 s. After blotting on Whatman filter paper 6 and air drying, the ultrathin sections were examined with TEM (JEM 2200 EX II, Tokyo, Japan) at a 200 KV field.

Alginate purification and quantification

After the designated incubation periods, extracellular alginate was isolated from the viscous cultures using the previously described method (Muhammadi and Shafiq, 2019). In summary, the crude CMG1418 alginate was dialyzed (tubing diameter 16 mm, Mr12, 400 Da) for 48 h, with periodic (16 h) water changes with distilled water (dH_2O). The dialyzed CMG1418 alginate was then dissolved in 5 ml of dH_2O, applied to a Sephadex G-75 column (75 × 1.6 cm), and eluted with double-distilled water (ddH_2O) at 0.4 ml/min. Fractions with a high Mol. wt that eluted in a single homogenous peak was collected, pooled, lyophilized (−50°C) under $70 × 10^{-3}$ MBAR, and recorded as pure alginate for downstream applications (Muhammadi and Ahmed, 2006). The alginate yield (%) from each culture was determined using Equation 1.

$$\text{Alginate yield } [\%] = \frac{\text{weight of alginate}}{\text{CDM}} \times 100 \quad (1)$$

Analytical methods

Fourier-transform infrared (FT-IR) analysis

Before analysis, a 20 mg aliquot of CMG1418 alginate was deacetylated in 5 ml of 0.3 N NaOH, as previously described (Muhammadi and Shafiq, 2019). For FT-IR

analysis, 400 µl of 4 mg/ml of both CMG1418 alginate and its deacetylated form were spotted onto polyethylene IR sample cards (3M, International Crystals Laboratories, Garfield, USA), dried in a laminar flow cabinet, and stored in a vacuum desiccator (PC-210KG, ProSciTech) for 24 h over P2O5. The analysis was performed using a Mattson GL-3020 Galaxy Series FT-IR 3000 Spectrometer operating over a range of 100–2000 cm^{-1}.

Acidic hydrolysis of alginate

Before NMR spectroscopy, 300 mg of CMG1418 alginate was partially hydrolyzed with hydrochloric acid (1 mol/l, pH 3) at 100°C for 1 h to reach a final average DP_n of approximately 30–40, as previously described (Muhammadi and Shafiq, 2019). The hydrolysate was cooled to 25°C, neutralized with 1.0 N NaOH, dialyzed for 24 h against dH_2O, and then lyophilized.

^{1}H-NMR spectroscopy

The partially hydrolyzed CMG1418 alginate was desalted using an EconoFit Bio-Gel P-6 desalting column (Bio-Rad), neutralized with 0.1 N NaOH, and then dissolved in 1 ml of D_2O. Five milligrams of the solution were freeze-dried and then redissolved in 0.5 ml of D_2O. Chemical shift reference was established by adding 20 µl of $C_6H_{13}NaO_2Si$ (0.3 M, Aldrich) directly to the sample tube. The spectra were recorded on an Avance DMX 500 spectrometer (Bruker, Karlsruhe, Germany) operating at 500 MHz. The molar fraction of G-residues (F_G) and its dimer (F_{GG}) was determined by measuring the area (A) under the anomeric peak region, using Equation 2. The M/G ratio, composition of (block structure) molar fractions of monomers (F_G and F_M), dimers (F_{MM}, F_{MG}, F_{GG}, and F_{GM}), and trimers (F_{GGG}, F_{GGM}, F_{MGM}, and F_{MMG}) were determined by integrating signals in the anomeric region (H-1) of the spectra, using Equations (3–11).

$$F_G = \frac{A_I}{A_{II} + A_{III}} \tag{2}$$

$$F_{GG} = \frac{A_{III}}{A_{II} + A_{III}} \tag{3}$$

The molar fraction of M was calculated as:

$$F_G + F_M = 1 \tag{4}$$

$$F_M = 1 + F_{MG} \tag{5}$$

The M/G ratio is defined explicitly as:

$$M/G = \frac{1 - F_G}{F_G} \tag{6}$$

The doublet frequencies relationships are given as:

$$F_{GG} + F_{GM} = F_G \tag{7}$$

$$F_{MM} + F_{MG} = F_M \tag{8}$$

The triplet frequency relationships are determined as follows:

$$F_{GGG} + F_{MGG} + F_{GGM} + F_{MGM} = F_G \tag{9}$$

$$F_{GM} = F_{GGM} + F_{MGM} = F_{MG} \tag{10}$$

$$F_{MGG} = F_{GGM} \tag{11}$$

The average DP_n was estimated by comparing the results of peak integration of the reducing-end units to the total spectrum signal intensity using Equation 12:

$$DP_n = \frac{M + G + red\alpha + red\beta}{red\alpha + red\beta} \tag{12}$$

To determine the degree of O-acetylation (DOA) at M-residues of CMG1418 alginate, the intensities (I) of acetyl protons were compared to those of unhydrolyzed alginate, corrected for the contribution of HOD (chemical shift of neat D_2O) using the equation ($I_{OAc}/3/(I_{Total}/5 - I_{HDO}$), as described by Skjåk-Bræk et al. (1986).

^{13}C-NMR spectroscopy

For the ^{13}C-NMR analysis, 100 mg/ml of partially hydrolyzed CMG1418 alginate was neutralized with 0.1 NaOH and dissolved in D_2O at pD 7. The ^{13}C-NMR spectra were recorded using an Avance II spectrometer (Bruker, Karlsruhe, Germany) operating at 125 MHz with 31.5 kHz spectral width and 64K data points. The spectra were accumulated from 4000 to 6000 scans at a pulse angle of 90° and a pulse repetition of 5.0 s under complete proton decoupling. The field-frequency lock was achieved using ^{2}H. The spectra were analyzed with the Bruker program 1D-WIN NMR provided by Bruker. The DP_n, M/G ratio, and M/G molar fractions were determined using methods described in ^{1}H-NMR analysis (Equations 2–12). The DOA was determined by comparing the integral of the methyl signal with that of any carbon position of the M unit using Equation 13.

Gel permeation chromatography (GPC)

To determine the relative Mol. wt, GPC was performed on Sephadex G-50 and G-100 columns (80 × 2.0 cm) obtained from Sigma-Aldrich. The chromatography was conducted using ddH_2O as the mobile phase, as described in a previous study by Muhammadi and Shafiq (2019). Before analyzing the CMG1418 alginate, the columns were calibrated using a range of broad dextrans

standards (T10, T20, and T250) (Sigma-Aldrich) to determine the void volume (V_o) and D-(+) glucose (Sigma-Aldrich) to determine the included volume (V_i).

Biocompatibility assessment of CMG1418 alginate

Hemolysis assay

Five healthy male volunteers aged 20–30 years provided blood samples (5 ml) that were collected in tubes containing 5.4 mg of EDTA. Prior written informed consent was obtained from the volunteers, and the study was conducted under the guidelines approved by the Bioethics Committee of the Centre for Bioresource Research, Islamabad, Pakistan, for research involving human subjects. Each blood sample was centrifuged at 1000 rpm for 10 min at 4°C, and the plasma was carefully removed by aspiration with a pipette. The red blood cells were washed three times with 1× phosphate-buffered saline (PBS) (pH 7.4) for 5 min and stored at 4°C until use (within 6 h).

An aliquot of 50 µl of 10 × (100 µl RBCs suspension: 900 µl 1× PBS) was mixed separately with 100 µl of alginate CMG1418, partially hydrolyzed alginate CMG1418, 100 µl of 1× PBS (negative control), and 100 µl of 1% SDS (positive control). Each reaction mixture was incubated at 37°C in a water bath for 60 min. The volume of the reaction mixture was made up to 1 ml by adding 850 µl of 1× phosphate buffer and centrifuged at 300 rpm for 3 min. The concentration of resulting hemoglobin in each supernatant was measured at 540 nm using a 96-well multiplate reader (Spectra MAX-340). The *in vitro* hemolytic assay was performed in triplicate for each test sample, and the percentage of hemolysis was calculated using Equation 13:

$$\text{Hemolysis [\%]} = \frac{\text{OD of sample} - \text{OD of PBS}}{\text{OD of SDS} - \text{OD of PBS}} \times 100 \quad (13)$$

Cell viability assessment by MTT assay

The MTT reduction assay, with minor modifications to the method described by Mosmann (1983), was used to measure cellular metabolic activity as an indicator of cell viability, proliferation, and cytotoxicity. The breast cell line MCF-7, trypsinized to 70–80% confluence, was incubated for 24 h at 37°C in a 5% CO_2 incubator. Both polymeric and partially hydrolyzed CMG1418 alginate samples were separately added to Dulbecco's Modified Eagle Medium (Thermo Fisher Scientific) without fetal

bovine serum and incubated for 24 h. After incubation with the test samples, the medium was removed from the wells and replaced with fresh medium. Following incubation with (3-(4,5-dimethylthiazol-2-yl)-2,5-diphenyl-tetrazolium bromide (MTT) reagent (Sigma-Aldrich), the medium was again removed from the wells, and 100 µl of DMSO was added to rapidly solubilize the formazan. The concentration of solubilized formazan was measured at 570 nm using a 96-well multiplate reader (Spectra MAX-340). To avoid possible false-positive or high viability values, the media in the treated cells was changed after 24 h, and the MTT assay was repeated. Tamoxifen (20 µM) and untreated cells were used as controls. The assay was repeated four times independently for each test sample and control, and the percentage of cell viability was estimated using Equation 14:

$$\text{Cell viability [\%]} = \frac{\text{mean OD of treated cells}}{\text{mean OD of control cells}} \times 100 \quad (14)$$

Analysis of functional properties of CMG1418 alginate

Determination of water absorption and retention capacities

To determine the water affinity of CMG1418 alginate, its capacities for absorption and retention were assessed using the teabag method with some modifications, as described by Kurane and Nohata (1994). One gram of each desiccated (at 110°C) CMG1418 alginate, Satialgine SG500 (high G) (Sanofi Bio-Industries, France), Sobalg FD120 (low G) (Sanofi Bio-Industries, France), cellulose, and xanthan were placed in separate empty teabags (Lipton Unilever, Pakistan) and immersed into dH_2O. To achieve the optimal absorption capacity, polymer samples were allowed to absorb water for stipulated periods (10, 20, 30, 40, 50, 60, 70, 80, 90, 100, 110, 120, and 130 min), and the water holding capacity was determined for 1, 2, 5, 10, 15, and 20 days at 10, 20, 30, 40, 50, and 60°C. Each experiment was repeated four times under the same conditions outlined above.

Determination of lipid emulsification activity

The emulsifying activity was evaluated using the method described by Kurane and Nohata (1991). Five milliliters of each edible vegetable oil, namely coconut oil (Medella, Malaysia), sunflower oil (Macjerry, Ukraine), and olive oil (Mueloliva, Spain), were added to separate test tubes containing equal volumes of CMG1418 alginate (0.5%). The mixture was homogenized using a homo-

genizer HG-15D (Witeg Lab, Germany) at 16 000 rpm for 3 min and centrifuged (5000 rpm) for 5–10 min. Similar experiments were carried out using control emulsifying agents, such as xanthan, arabic gum, locust bean gum, and alga alginates (Satialgine SG500, Satialgine SG300, Sobalg FD170, and Sobalg FD120) (Sanofi Bio-Industries, France), and dH_2O. After centrifugation, the heights of the emulsified and whole layers were measured. Each sample was tested four times independently under the same experimental conditions, and the emulsification index was calculated using Equation (15):

$$\text{Emulsification index [\%]} = \frac{\text{height of emulsified layer}}{\text{height of whole layer}} \times 100 \qquad (15)$$

Measurement of flocculation activity

To determine the flocculating activity, the turbidity of a kaolin clay suspension was measured using the method described by Kurane and Nohata (1991). In a 100 ml beaker, a 40 ml suspension of kaolin clay (5 g/l, pH 7) was mixed with 4 ml of $CaCl_2$ (1%, pH 7), and 1 ml of CMG1418 alginate (1 ml, 1%, pH 7) for 1 min on a stirring hot plate and left for 5 min at ambient temperature. In addition to CMG1418 alginate, commercial algal alginates, such as Satialgine SG500 (high G), Satialgine SG300, Sobalg FD170, and Sobalg FD120, were also tested for flocculation under the same experimental conditions in four independent replicates. The optical density of the supernatant and negative control (without alginate) was measured at 550 nm using a 96-well multiplate reader (Spectra MAX-340). The flocculation index (%) was calculated using Equation (16):

$$\text{Floculation index [\%]} = \left(\frac{1}{A} - \frac{1}{B}\right) \times 100 \qquad (16)$$
$$A = \text{absorbance of the sample}$$
$$B = \text{absorbance of the control}$$

pH-stability, cationic-stability, and thermo-stability of flocculating activity

Both algal and CMG1418 alginates (5 mg/ml) were separately dissolved in dH_2O, divided into ten equal volumes (10 ml), and adjusted over a wide range of pH (3–12). Each solution was stored in a refrigerated incubator (Thermo Scientific) at 4 °C for 24 h, and the residual flocculating efficiencies were measured at ambient temperature. To investigate the effect of cations, alginate solutions were treated with different concentrations

(0.1–5%) of NaCl, KCl, $CaCl_2$, $MgCl_2$, $FeCl_3$, and $Al_2(SO_4)_3$. For the thermal stability test, each alginate solution (5 ml) was heated (50–100 °C) for 60 min, and the flocculating activity was measured at pH 7.0.

Test for gel formation

Solutions of CMG1418 alginate (1–3%), 1% agar agar (Difco), and algal alginate Satialgine SG500 were separately heated at 50, 60, 80, 100, 115, and 121 °C for 1–2 min and allowed to cool (10–30 °C) for gelling. The effect of pH on gelling was tested by adjusting the solutions to pH 2–12. The effect of cations on gel formation was determined by heating the solutions of test samples with different concentrations (0.1–5%) of $CaCl_2$, $MgCl_2$, NaCl, and KCl under similar conditions as described above. Each test sample solution was subjected to gel formation under identical experimental conditions in four independent replicates, and the results are expressed as mean ± SEM.

Measurement of viscosity

Solutions (1%) of CMG1418 alginate and commercial algal alginates Satialgine SG-500 and Sobalg FD-120 were adjusted to pH 2–12 using HCl (1.0 N) and NaOH (1.0 N). Absolute viscosities were measured using a Wells-Brookfield cone/plate viscometer (LVDV-1), with cone sizes CP-46 (<5000 cP) and spindle speeds (5, 10, 20, 50, and 100 rpm) at 25, 50, 60, and 90 °C. Fluid viscosities were calculated according to the manual of Wells-Brookfield and expressed in units of cP. Under similar conditions, absolute viscosities of each test sample were measured from four independently repeated experiments and expressed as mean ± SEM.

Statistical analysis

The numerical data obtained from four independently repeated experiments of each *in vitro* and other parametric assays were analyzed using One-way ANOVA with the Statistix 8.1 software at a significance level of $P < 0.05$. The results are shown as mean ± SEM.

Results and discussion

Seasonal, temporal, spatial, species-specific, and organ-specific variations in chemical composition and content, drying, and extraction methods are known to cause inconsistencies in the characteristic functional properties and application of currently used alginates from sea-
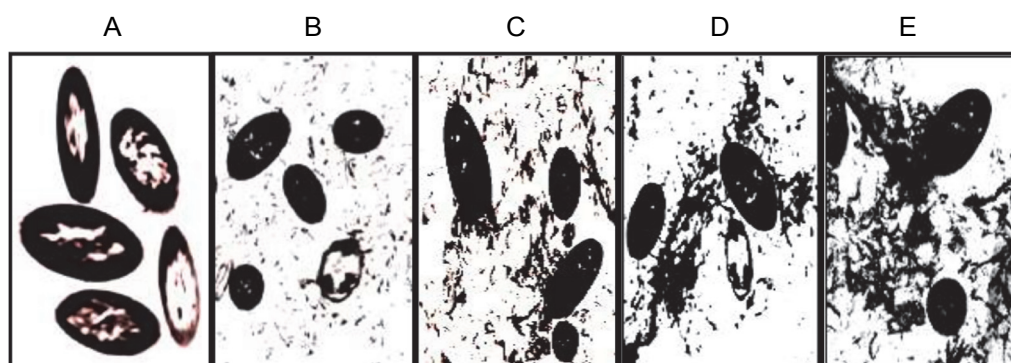
Fig. 1. Transmission electron micrographs A–E showing the biosynthesis and transport of extracellular alginate by *P. aeruginosa* CMG1418 at 12, 24, 48, 72, and 120 h, respectively

weeds and synthetic sources (Arunkumar, 2017; Fertah et al., 2017; Valentine et al., 2020). Additionally, there are no previous reports on the structural characterization of alginate with an abundance of M residues (M-blocks) lacking poly-G from a bacterial source, nor on the investigation of promising functional properties for viscosifying, flocculating, emulsifying, and water-absorbing and water-retaining applications. In this study, alginate synthesized by *P. aeruginosa* CMG1418 was physiochemically investigated to address these issues. This is the first report on the unique functional potential of bacterial alginate, which has the potential to resolve these inconsistencies by substituting commercial alginates with structurally unique and consistent bacterial alginate.

Identification of bacterial strain

A 558 bp DNA fragment was amplified from the genomic DNA of *P. aeruginosa* CMG1418 and subsequently sequenced. BLAST analysis of these sequences showed a 90–100% homology (BLAST results of GenBank Accession No: EF210102 at NCBI search) with the 16S rRNA gene sequences of several reported *P. aeruginosa* strains available in GenBank, EMBL, DDBJ, and PDB, as well as rRNA homology group I *Pseudomonas* (Fialho et al., 1990; Eremwanarue et al., 2021). Based on the 16S rRNA gene sequence homology (100%), the bacterial strain CMG1418 isolated from contaminated soil in the food industry was identified as *P. aeruginosa*.

Transmission electron microscopy

TEM analysis revealed that cells of *P. aeruginosa* were heavily stained with RR due to the presence of acidic polysaccharide (alginate) in the intracellular peri-

plasmic spaces and cell wall (Fig. 1). In addition, it was observed that negatively RR-stained alginate was secreted from cells of cultures older than 12 h into the extracellular environment outside the cell wall, with the amount increasing proportionally with longer incubation periods (Fig. 1B–E). These findings demonstrated that newly synthesized acidic polysaccharide alginate in the intracellular periplasmic spaces was gradually transported into the extracellular medium. These results are consistent with previous reports indicating that the polymer synthesized inside the bacterial cell at periplasm is then transported out of the cell into the surrounding environment by a porin-like multiprotein complex spanning from the inner to the outer membrane as a partially insoluble slime or loosely attached to the cell surface (Madilyn and Floodgate, 1973; Sabra et al., 2000).

Furthermore, the RR-specific staining of acid polysaccharides in both intracellular and extracellular media revealed the structural organization of supplied sucrose into large Mol. wt acidic exopolysaccharide with the incubation period. Therefore, the results from TEM analysis confirmed that the slime produced by *P. aeruginosa* is the acidic exopolysaccharide alginate (Carlson and Matthews, 1966; Ogle et al., 1987; Hills et al., 2021), which is also true for CMG1418 alginate biosynthesis in this study.

Quantification of cell growth and alginate biosynthesis

Table 1 showed that among cultures grown for different incubation periods, the maximum yield of alginate with 100.00% total UA was obtained after 120 h, which was equivalent to 20% of the total supplied sucrose carbon source. No extracellular alginate was produced

Table 1. Quantification of growth and alginate synthesized by *P. aeruginosa* CMG1418

| Incubation period [h]	CDM [mean ± SD g/l]	Alginate [mean ± SD% w/w CDM]	Alginate [mean ± SD g/l]
0	0	0	0
12	0.015 ± 0.002	0	0
18	0.087 ± 0.005	0	0
24	0.286 ± 0.003	5.244 ± 0.013	0.015 ± 0.004
48	1.053 ± 0.001	42.070 ± 0.015	0.443 ± 0.005
72	2.068 ± 0.003	122.147 ± 0.004	2.526 ± 0.016
120	2.355 ± 0.002	172.186 ± 0.003	**4.055 ± 0.05**
150	2.354 ± 0.004	172.132 ± 0.011	4.052 ± 0.013
170	2.351 ± 0.004	170.77 ± 0.013	4.015 ± 0.002
300	2.346 ± 0.013	162.02 ± 0.006	3.801 ± 0.005
360	2.341 ± 0.013	142.503 ± 0.002	0.005
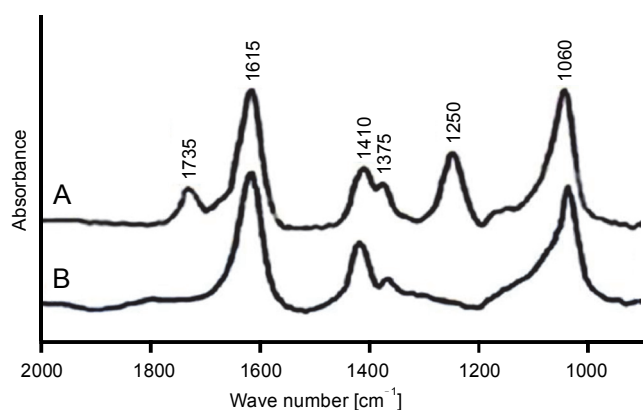
Fig. 2. Comparison of stacked FT-IR spectra of (A) acetylated and (B) deacetylated CMG1418 alginate, respectively

during the first 18 h of incubation, but there was an increase in CDM (0.057 ± 0.005 g/l) (Table 1). However, both yield and CDM were positively correlated with the incubation period from 18 to 120 h. After 150 h, there was no further increase in alginate yield (Table 1), but a gradual reduction in yield with a slower rate of decreasing CDM was observed (Table 1). This indicated a proportional correlation between alginate yield and the number of cells. These results also suggested that nutrients, including the carbon source, were available for sustainable growth and alginate production up to 150 h after which prolonged incubation led to a reduction in yields due to nutrient scarcity (Manresa et al., 1987).
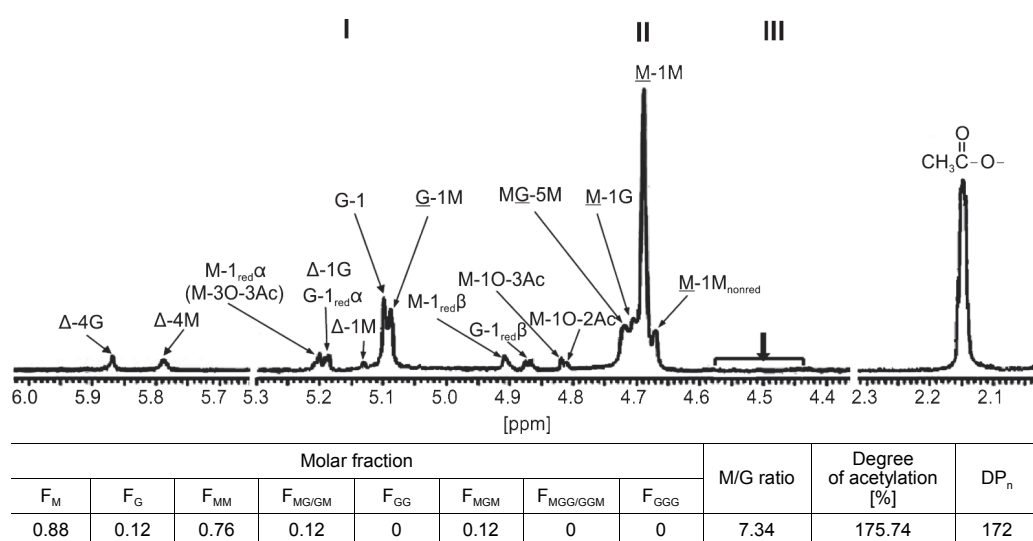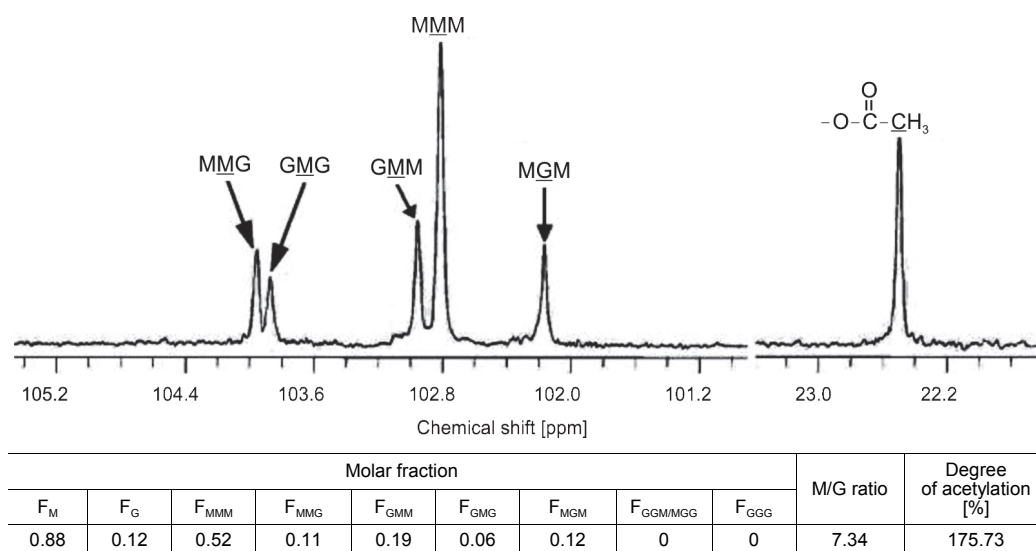
Therefore, to sustain their exhausted growth, surviving cells might have degraded the alginate into oligo-saccharides of respective constituents as a consumable carbon source using extracellular alginate lyase (Koti et al., 2014).

Structural characteristics of CMG1418 alginate

Functional groups

The FT-IR spectrum of purified alginate exhibited absorbance peaks at six different regions, while the deacetylated alginate had only four peaks (Fig. 2A, Fig. 2B). The bands at 1060 cm^{-1} in both acetylated and deacetylated alginates were assigned to C–OH and O–H stretching, indicating the presence of hydroxyl groups in alginate monomers (Franklin and Ohman, 2002; Muhammadi and Shafiq, 2019). The peaks at 1375 and 1410 cm^{-1} represented the symmetric and asymmetric stretching behavior of carboxylate (O–C–O) vibration, respectively, suggesting the presence of carboxylic group (COO$^-$) in M-residue and G-residue of alginate (Anastassiou et al., 1987; Meena et al., 2020). The bands observed at 1250 and 1735 cm^{-1} were due to C–O–C and C=O stretching of ester bonds in acetyl groups, respectively (Fig. 2A), which were not detected in alkali-treated CMG1418 alginate (Fig. 2B) due to alkaline deacetylation (Franklin and Ohman, 1996). These results suggested the presence of O-acetyl groups linked to the M-residues of CMG1418 alginate (Usov, 1999; Ertesvåg, 2015). The results of FT-IR were consistent with previous similar reports on alginate from *P. aeruginosa* (Franklin and Ohman, 1996; Nivens et al., 2001; Moradali et al., 2015).

Molar fraction								M/G ratio	Degree of acetylation [%]	DP$_n$
F$_M$	F$_G$	F$_{MM}$	F$_{MG/GM}$	F$_{GG}$	F$_{MGM}$	F$_{MGG/GGM}$	F$_{GGG}$			
0.88	0.12	0.76	0.12	0	0.12	0	0	7.34	175.74	172

Fig. 3. ^{1}H-NMR spectra of partially hydrolyzed CMG1418 alginate

Molar fraction									M/G ratio	Degree of acetylation [%]
F$_M$	F$_G$	F$_{MMM}$	F$_{MMG}$	F$_{GMM}$	F$_{GMG}$	F$_{MGM}$	F$_{GGM/MGG}$	F$_{GGG}$		
0.88	0.12	0.52	0.11	0.19	0.06	0.12	0	0	7.34	175.73

Fig. 4. ^{13}C-NMR spectra of partially hydrolyzed CMG1418 alginate

Monomer composition and distribution

Figure 3 shows the ^{1}H-NMR spectra, which exhibited strong signals of chemical shift at 5.1, 5.09, 4.73, 4.71, and 4.69 ppm, indicating the specific peak for G-anomeric proton (G-1), G-H-1 of alternating GM-block (G-1M), H-5 of alternating MG-blocks (GM-5), M-H-1 of alternating MG-block (M-1G), and anomeric proton (M-1) of poly-M (M-block) in CMG1418 alginate, respectively. However, there were no characteristic signals observed that might be arising from H-5 of GG-5M (4.74–4.78 ppm), GG-5G (4.45–4.58 ppm), and MG-5G (4.38–4.44 ppm) (Grasdalen, 1983; Fertah et al., 2017). These results indicated that CMG1418 alginate also did not contain poly-G-blocks in its structure similar to that from other *Pseudomonas* spp. (Fyfe and Govan, 1983; Muhammadi and Shafiq, 2019). The integration of the signals in the anomeric region showed that the alginate was composed of 88% M and 12% G residues, giving an M/G ratio of 7.34. Therefore, the ^{1}H-NMR analysis revealed that the CMG1418 alginate was composed of 76% poly-M-block, 12% alternating MG/GM-block, and 12% MGM-block, lacking any conspicuous poly-G-blocks.

The ^{1}H-NMR spectrum also showed that the signals appearing at the anomeric regions indicated the linkage between G/M and M-blocks (Grasdalen, 1983; Heyraud et al., 1996). Further, the strong signals of a chemical shift that appeared at the M-1M and M-1G were assigned to anomeric proton (H-1) configuration of an M-residue and adjacent to another M-residue or a G-residue, respectively (Fig. 3). Similarly, the chemical shift signals that appeared at MG-5M region were assigned to the H-5 of the central G-residue in an MGM triad, while that at G-1M referred to the corresponding signals of the anomeric proton (H-1) of G-residue immediately adjacent to M-residue in MG-blocks (Fig. 2).

In the ^{1}H-NMR spectrum, there were weak resonance signals at 4.68, 4.87, 4.91, 5.13, 5.19, 5.20, 5.79, and 5.87 ppm, indicating signals from M-1$M_{nonred}\alpha$, G-1$_{red}\beta$, M-1$_{red}\beta$, Δ-1M, G-1$_{red}\alpha$/Δ-1G, Δ-G, and Δ-4M, respectively, resulting from partial acid hydrolysis of alginate for ^{1}H NMR analysis (Fig. 3). These findings indicated that the M–M glycoside bonds in poly-M-block in CMG1418 alginate, when partially hydrolyzed, produced the M_{red} at the reducing end and ΔM at the nonreducing end (Bjerkan et al., 2004a; Kam et al., 2011).

When the M–G glycoside bond in the MG-block was partially hydrolyzed, it produced M_{red} on the reducing end and ΔM or ΔG on the nonreducing end, as shown in Fig. 3. On the other hand, when the G–M glycoside bond in the MG-block was hydrolyzed, it resulted in G_{red} on the reducing end and ΔG or ΔM on the nonreducing end (Bjerkan et al., 2004; Kam et al., 2011). The high-resolution ^{13}C-NMR spectrum of partially hydrolyzed CMG1418 alginate also revealed the trimers (F_{GGG}, F_{MGM}, F_{GGM}, and F_{MGG}) in the CMG1418 alginate block structure (Fig. 4). The C-1 signal spectral resolution displayed resonance peaks for the four M-centered triads MMM (102.82 ppm), GMM (102.96 ppm), GMG (103.88 ppm), and MMG (103.96 ppm), and one G-centered triad MGM (102.17 ppm). The signals specific for GGM (102.18/103.07–103.22 ppm), GGG (103.25–103.6 ppm), and MGG (103.35/104.19–104.37 ppm) were not detected except for one G-centered triad MGM (102.17 ppm), indicating the complete absence of consecutive G residues or poly-G-blocks, as reported for alginates from *Pseudomonas* species (Remminghorst and Rehm, 2006; Urtuvia et al., 2017).

The integration of the intensities of observed C-l multiplet signals yielded the distribution of the triplet
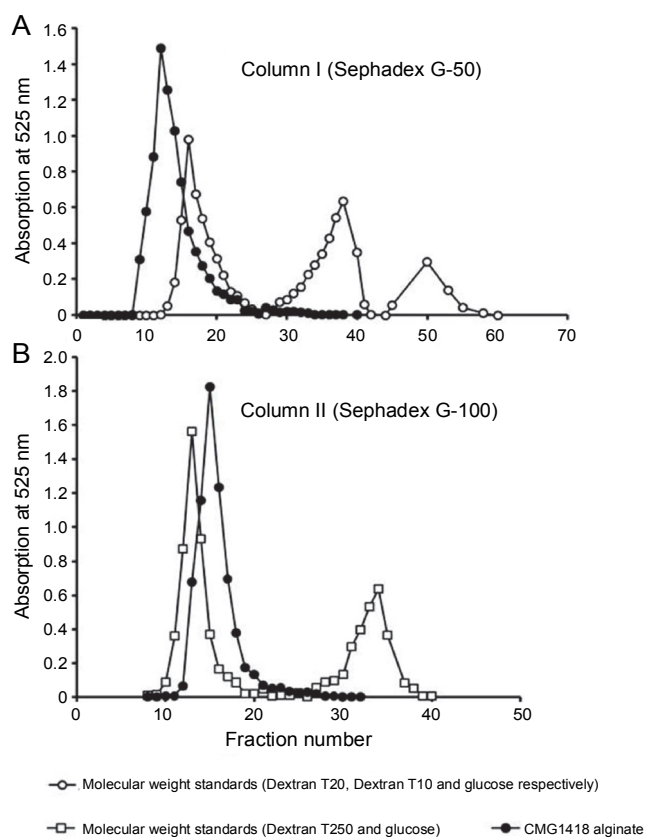

Fig. 5. Gel permeation chromatographic elution profile of CMG1418 alginate from Sephadex G-50 and G-100

frequencies of M and G residues and their molar ratio. These data on the chemical composition and sequential parameters of the polymeric chain structure are consistent with previous reports on alginate from *P. aeruginosa* and with that determined by ^{1}H-NMR in this study (Fig. 4) (Narbad et al., 1990; Schürks et al., 2002). By comparing the resultant peak integration of the reducing-end units (redα and redβ) to the total spectrum signal intensity, the average DP_n was estimated to be 172, giving an average Mol. wt of polymeric alginate of 46 500 Da or g/mol, which falls within the Mol. wt range of > 20 000 and < 250 000 Da determined by GPC (Fig. 5A) and is in agreement with previous reports on the Mol. wt of alginates produced by *P. aeruginosa* (Kam et al., 2011; Goh et al., 2012; Muhammadi and Shafiq, 2019).

O-acetylation of polymeric mannuronates

The ^{1}H-NMR spectra presented in Figure 3 showed weak resonance signals at 4.81, 4.82, and 5.24 ppm, which were attributed to H-1O-2Ac, H-1O-3Ac, and H-3O-3Ac associated with O-2 and O-3 of M units. The ^{1}H-NMR spectra showed a strong signal at 2.15 ppm, which was

Table 2. Cytotoxic activities of polymeric and partially hydrolyzed CMG1418 alginate

Treatment	Concentration [µg/ml]	Hemolysis [%]	Cell viability [%]
Polymeric CMG1418 alginate	10	0	100.02 ± 0.13
	20	0	100.00 ± 0.21
	50	0	100.02 ± 0.03
	100	0	100.01 ± 0.11
Partially hydrolyzed CMG1418 alginate	10	0	100.00 ± 0.02
	20	-1.02	100.01 ± 0.05
	50	0	100.00 ± 0.04
	100	-1.00	100.30 ± 0.12
PBS	1 X	0	
SDS	1%	92.55 ± 0.14	
Tamoxifen	20 µM		30.03 ± 0.02
Untreated cells			100.00 ± 0.00

attributed to –CH_3 of O-acetyl group (Fig. 3). The integration value of the methyl signals (5.24, 4.82, 4.81, and 2.15 ppm) of acetyl groups indicated 175.74% of acetyl substituent to each of the anomeric signals from M-residues, suggesting two O-bound acetyl groups per each M unit (Fig. 3). Based on this observation, the mannuronate-to-O-acetyl ratio was estimated to be 2.0, indicating that the M residues were di-O-acetylated, likely at O-2 and O-3 positions on the sugar ring (Skjåk-Bræk et al., 1986; Bjerkan et al., 2004b).

Similarly, Figure 4 showed that the strong ^{13}C-signals at 22.45 ppm in the high field region indicated the presence of methyl groups in acetyl residues of M units. The comparison of the integral of the methyl signal with that of any carbon position of M unit showed 175.73% of acetyl substituent, which also suggested the presence of two O-bound acetyl groups/M unit (Fig. 4) (Schürks et al., 2002). Thus, ^{1}H-NMR and ^{13}C-NMR analysis confirmed that the polymeric chain of CMG1418 alginate had a DOA of two acetyl groups per each mannuronate unit.

Previous studies have shown that the DOA of alginate has an inverse linear relationship with the maximal specific growth rate over the range of 20–35°C and might reflect the availability of acetyl-CoA precursors (Leitào et al., 1992). The slower-growing cells exhibit higher acetyl content, and the degree of acetylation could reflect acetyl-CoA availability, considering the precursor acetyl-CoA as the probable source of acetyl in the final polymer (Sutherland, 1990). These reports support the findings of this study on the biosynthesis of di-O-acetylated alginate by *P. aeruginosa* CMG1418, which attained the maximum growth and polymer yield at 30°C (Table 1), falling within the range (20–35°C) reported for the maximal specific growth rate and O-acetylation.

Relative molecular weight and its distribution

The GPC profile revealed that a majority of the applied CMG1418 alginate (98.832% UA) was eluted from Sephadex G-50 column I in a homogenous major peak before V_o, with an apparent relative Mol. wt range of > 20 000 Da (Fig. 5A). However, a small fraction (1.23% UA) of alginate was also eluted within V_o, which could be low Mol. wt polyuronides or oligouronides. Additionally, due to their stereochemistry, some of the alginate molecules might have adhered to the column gel, and as a result, they could not elute with the high Mol. wt alginate and lagged (Muhammadi and Ahmed, 2006). Furthermore, Figure 4B indicated that the entirety of the applied CMG1418 alginate was eluted from Sephadex G-100 column II in a single homogenous peak (100.063% total UA) just after the V_o, indicating a Mol. wt, < 250 000 Da. Therefore, the GPC elution profiles demonstrated that CMG1418 alginate had a relative dispersion of Mol. wt (> 20 000 and < 250 000 Da) which agreed with the average DP_n determined by ^{1}H-NMR (Fig. 3) and ^{13}C-NMR (Fig. 4). Moreover, this Mol wt. range was consistent with previously reported bacterial

alginates (Moradali et al., 2015; Urtuvia et al., 2017). Consequently, the MG ratio, molar fractions of monomers of each alginate block structure, DOA and DP_n, determined through ^{1}H-NMR, ^{13}C-NMR analysis, and relative Mol. wt suggested that the composition of CMG1418 alginate was similar to that of MM-blocks-dominated alginates from *Pseudomonas* species (Moradali et al., 2015; Bai et al., 2017; Urtuvia et al., 2017).

Assessment for cytotoxicity and biocompatibility

In this study, CMG1418 alginate was tested for cytotoxicity and biocompatibility to ensure its safe future utilization, especially in pharmaceutical and healthcare applications. Interestingly, both the polymeric CMG1418 alginate and its partial acid hydrolysate were found to be nonhemolytic to RBCs, similar to the negative control PBS (Table 2). Similarly, the MTT assay revealed that none of the test concentrations of CMG1418 alginate and its partial acid hydrolysate inhibited the proliferation of the MCF-7 cell line, and the proliferating cells were 100% viable with active metabolism similar to untreated cells ($P > 0.05$) (Table 2). Since CMG1418 alginate did not show any cytotoxic or antimetabolic activities, these results provide experimental evidence of its biocompatible, nonimmunogenic, and nontoxic nature for safe use (Sachan et al., 2009; Dudun et al., 2022).

Functional properties of CMG1418 alginate

Water absorption and retention capacities

The study found that CMG1418 alginate was able to absorb water up to 375 times its dry weight within 60 min, which was significantly faster than algal alginates, xanthan, and cellulose, which required 100–120 min to achieve their maximum water absorption capacities (Fig. 6). Once CMG1418 alginate reached its maximum capacity, it maintained a constant absorption plateau (Fig. 6). Moreover, the alginate was able to retain 45% of supplied water for 30 days under hot (60 °C) desert environmental conditions, without any further loss of water after day 15 (Fig. 6). In comparison, algal alginates, cellulose, and xanthan could only retain 6, 4, 7 and 5% of supplied water, respectively (Fig. 7).

The researchers attributed the strong water-absorbing ability of CMG1418 alginate to its polymeric acidic nature and high Mol. wt, which allowed it to establish a hydrophilic interaction with water (Kurane and Nohata, 1994; Moscovici, 2015). These results were further
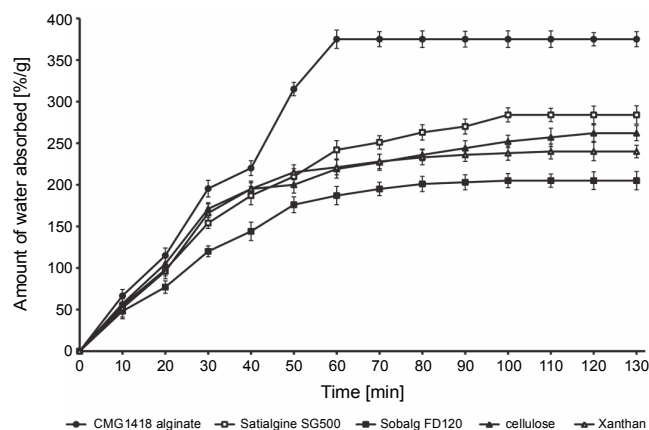

Fig. 6. Optimum water absorption capacities of hydrophilic polysaccharides
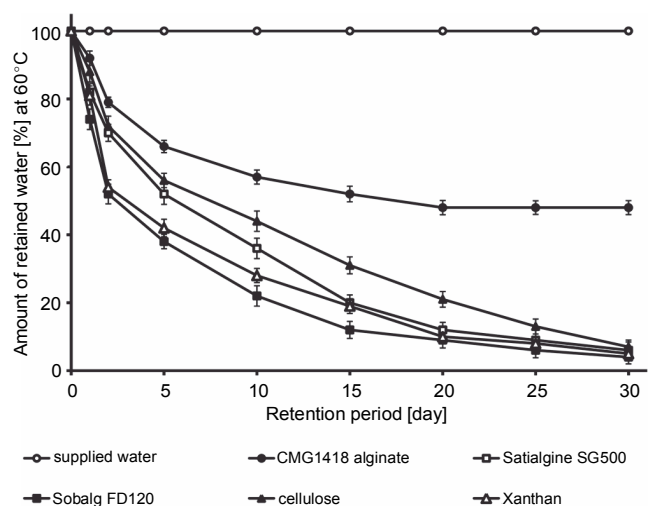

Fig. 7. Optimum water retention capacities of hydrophilic polysaccharides

substantiated by previous reports that O-acetyl groups associated with CMG1418 alginate increased the water-binding capacity and significantly influenced the physiochemical properties of the polymer, such as the water-binding capacity as well as the viscosity, and the ability to bind divalent cations (Skjåk-Bræk et al., 1989; Brzezińska and Szparaga, 2015).

Considering its significantly stable water-absorbing (up to several hundred times its weight) and retaining capacities, CMG1418 alginate could be a suitable and ecofriendly substitute for other natural water-absorbing agents, such as cellulose, xanthan, and algal alginates.

Emulsifying activity of CMG1418 alginate

The emulsion stability of the three commonly used vegetable edible oils and CMG1418 alginate was found to remain intact after centrifugation (5000 rpm), in-

Table 3. Comparative lipid emulsifying activity of CMG1418 alginate

Emulsifying agent [0.5%]	Emulsification index [%]		
	coconut oil	sunflower oil	olive oil
CMG1418 alginate	99.00 ± 0.16	100.0 ± 0.01	99.68 ± 0.03
Xanthan	85.00 ± 1.03	90.00 ± 1.07	86.45 ± 0.22
Satialgine SG500	76.00 ± 1.10	78.00 ± 0.15	80.38 ± 1.05
SG300	72.40 ± 0.13	72.60 ± 0.08	73.05 ± 0.23
Sobalg FD170	32.16 ± 0.21	33.24 ± 0.13	33.17 ± 1.16
FD120	28.20 ± 0.05	29.04 ± 0.18	29.55 ± 1.04
Locust bean gum	42.00 ± 0.14	50.00 ± 1.06	53.52 ± 0.14
Arabic gum	12.00 ± 0.17	23.76 ± 1.02	28.00 ± 0.08
Water	0	0	0

dicating its effectiveness as an emulsifier (Table 3). In comparison to other commercially used oil emulsifying agents such as xanthan, locust bean gum, and arabic gum, as well as algal alginates (Satialgine SG500, Satialgine SG300, Sobalg FD170), CMG1418 alginate exhibited higher potential for emulsification (99–100%) of vegetable edible oils, suggesting its strong and irreversible amphiphilic affinity (Table 3). This is due to the asymmetric nature of M monomers in the polymeric chains, which display distinct hydrophilic and hydrophobic surfaces on opposite sides, resulting in stable emulsification (Stewart et al., 2017).

In comparison to algal alginates and other commercially available emulsifying agents, CMG1418 alginate demonstrated higher emulsifying activity (Table 3). Additionally, bacterial alginates are nontoxic and have been approved by the US Food and Drug Administration and WHO for human consumption and therapeutic purposes, making them a promising substitute for algal alginates in various industrial applications such as puddings, gelled meats, dense syrups, ice cream, toothpaste, relishes, salad dressings, and tart sources (MacDowell, 1974; Yalpani and Sandford, 1987; Moscovici, 2015).

Flocculating activity of CMG1418 alginate

The flocculation activity of CMG1418 alginate was found to be greatly affected by pH, temperature, and cations (Table 4). CMG1418 alginate displayed stable flocculating activity (85%) over a wide range of temperatures (20–100°C) and pH values (4–11), while pH values <4 and >11 led to a slight decrease in the degree of flocculation. Among the tested pH values (4–11), the highest flocculation (90.47%) was achieved at pH 9 (Table 4). The addition of divalent ($CaCl_2$ and $MgCl_2$) and trivalent cations ($Al_2(SO_4)_3$ and $FeCl_3$) slightly increased the flocculation activity by 5 and 8%, respectively, while the addition of monovalent cations reduced the flocculation efficiency of CMG1418 alginate. Therefore, the highest flocculating activity was achieved at 30°C and pH 9.0 with the addition of trivalent cations. In contrast, algal alginates exhibited poor and thermodynamically unstable flocculation activities (<49%) over a wide range of pH and temperature values, as well as with divalent and trivalent cations (Table 4). These results indicated that CMG1418 alginate consistently demonstrated high flocculation efficiency over a wide range of temperatures and pH values, especially with divalent and trivalent cations at 30°C and pH 9.0. The thermal flocculating stability of CMG1418 alginate was attributed to the core backbone of the polymer chain, high Mol. wt, DP_n, O-acetylation of M-residues, emulsifying activity, capability of forming viscous solutions at low concentrations, and high content of alcoholic groups on the polymeric chains. These properties suggested the flocculation mechanism proposed by Ruehrwein and Ward (1952) and Michaels (1954) for the aggregation of clay particles by CMG1418 alginate. In this study, the colloids functioned by adsorbing on the hydrated surface of the particles and bridging between the suspended particles, resulting in subsequent aggregation or flocculation. The adsorption occurred via hydrogen bonding between the hydroxyl and nonionized carboxyl groups of alginate and the hydroxyl group of the clay particles.

Table 4. Comparative flocculation characteristics of CMG1418 alginate

Parameters		Flocculation activity [%] of alginates [1%]				
		CMG1418	SG-500	SG300	FD170	FD-120
Temperature [°C]	10	45.47 ± 0.14	27.03 ± 0.12	24.00 ± 0.13	11.22 ± 0.12	09.44 ± 0.02
	20	73.55 ± 0.52	32.00 ± 0.25	26.40 ± 0.15	15.17 ± 0.15	12.25 ± 0.15
	30	86.55 ± 0.24	47.00 ± 0.14	35.65 ± 0.04	27.34 ± 0.02	22.00 ± 0.21
	50	85.87 ± 0.16	44.20 ± 0.05	43.00 ± 0.14	31.56 ± 0.18	17.32 ± 0.05
	60	84.84 ± 0.05	39.00 ± 0.43	35.40 ± 0.15	26.12 ± 0.05	16.25 ± 0.05
	80	84.65 ± 0.17	29.50 ± 0.50	28.00 ± 0.01	23.05 ± 0.14	14.00 ± 0.50
	90	78.45 ± 0.62	27.00 ± 0.13	26.00 ± 0.11	21.22 ± 0.12	12.56 ± 0.14
	100	77.69 ± 0.33	26.54 ± 0.04	24.70 ± 0.31	19.15 ± 0.05	10.30 ± 0.05
	115	64.23 ± 0.12	23.00 ± 0.05	20.44 ± 0.10	14.15 ± 0.32	10.01 ± 0.12
	121	32.52 ± 0.03	18.00 ± 0.15	15.30 ± 0.05	09.34 ± 0.17	09.14 ± 0.50
pH	2	13.34 ± 0.05	07.00 ± 0.15	06.00 ± 0.13	05.42 ± 0.15	05.07 ± 0.15
	3	37.23 ± 0.12	08.00 ± 0.05	08.50 ± 0.17	06.50 ± 0.05	06.20 ± 0.02
	4	70.57 ± 0.07	15.00 ± 0.15	14.50 ± 0.15	09.45 ± 0.05	08.50 ± 0.15
	5	74.05 ± 0.15	35.00 ± 1.00	33.00 ± 0.25	15.15 ± 0.15	12.00 ± 0.23
	6	78.76 ± 0.08	38.50 ± 0.06	36.05 ± 0.17	24.05 ± 0.15	20.25 ± 0.13
	7	86.45 ± 0.05	45.00 ± 0.06	43.00 ± 0.13	28.34 ± 0.05	25.47 ± 0.08
	8	88.53 ± 0.21	47.45 ± 0.12	45.00 ± 0.11	31.15 ± 0.16	29.35 ± 0.06
	9	89.76 ± 0.15	45.00 ± 0.23	43.00 ± 0.03	27.72 ± 0.03	23.45 ± 0.01
	10	85.08 ± 0.07	41.00 ± 0.50	39.30 ± 0.14	22.15 ± 0.15	21.45 ± 0.05
	11	74.36 ± 0.11	32.50 ± 0.15	28.00 ± 0.05	19.00 ± 0.05	18.33 ± 0.22
	12	67.70 ± 0.04	25.00 ± 0.12	22.55 ± 0.13	10.00 ± 0.03	11.00 ± 0.15
Cations [0.1–3%]	$Al_2(SO_4)_3$	98.78 ± 0.11	42.00 ± 0.05	40.50 ± 0.02	31.23 ± 0.05	30.80 ± 0.13

These results indicated that CMG1418 alginate might be useful in neutral, basic, and acidic conditions to reduce turbidity, and could be a potential substitute for conventional flocculants in downstream processing of food, fermentation industries, and water treatment (Tawila et al., 2018).

Gelling properties CMG1418 alginate

In comparison to commercially available gelling agents agar agar (1%) and algal alginate (1% SG-500), solutions (1–3%) of CMG1418 alginate were unable to form strong gels across a broad range of temperature and pH strengths, despite the presence of divalent and trivalent cationic crosslinking agents, but instead formed soft to elastic flexible gels (Table 5). However, the addition of divalent ($CaCl_2$ and $MgCl_2$) and trivalent cations ($Al_2(SO_4)_3$ and $FeCl_3$) could slightly improve the forma-

tion of elastic to flexible gels, while monovalent cations had a negative impact on the gelling ability (Table 5). The gel-forming ability of alginates is primarily dependent on factors such as polymer chain length, composition, sequence, M/G ratio, and concentration of cross-linking agents, whereas the gel strength is dependent on the content and length of G-blocks, which have a higher affinity towards cationic crosslinkers than alginates with high M content (Mancini et al., 1999; Goh et al., 2012; Fertah et al., 2017). As a result, alginates with higher content of M-residues and M/G-mixed sequences can form relatively weaker or more flexible gels (Drage and Taylor, 2011). Additionally, the O-acetylation of M-residues has been found to reduce the affinity of alginate for cations (Skjåk-Bræk et al., 1989). In the present study, CMG1418 alginate formed soft to elastic flexible gels due to a lower degree of cross-linking caused by the ab-

Table 5. Comparative rheological characteristics of CMG1418 alginate [1 %]

Parameters		Viscosity [cP]			Gelling [g/cm^2]		
		CMG1418	FD-120	SG-500	CMG1418	Agar agar	SG-500
Temperature [°C]	10	4300.00 ± 0.13	34.00 ± 0.15	45.03 ± 0.42	9.34 ± 0.12	23.64 ± 0.05	15.42 ± 0.12
	20	4500.00 ± 0.14	46.50 ± 0.12	55.00 ± 0.22	12.53 ± 0.14	38.27 ± 0.13	23.52 ± 0.02
	30	4500.00 ± 0.11	105.00 ± 0.05	310.00 ± 0.10	22.23 ± 0.32	82.54 ± 0.17	46.55 ± 0.24
	50	4500.00 ± 0.10	105.00 ± 0.04	300.20 ± 0.05	27.22 ± 0.13	151.43 ± 0.03	85.32 ± 0.15
	60	4500.00 ± 0.13	100.40 ± 0.05	290.00 ± 0.32	30.16 ± 0.08	160.27 ± 0.32	94.55 ± 0.22
	80	4500.00 ± 0.12	95.00 ± 0.06	275.50 ± 0.52	33.31 ± 0.15	197.33 ± 0.50	104.65 ± 0.17
	90	4500.00 ± 0.10	90.00 ± 0.21	250.00 ± 0.35	34.24 ± 0.13	215.51 ± 0.14	121.45 ± 0.43
	100	4500.00 ± 0.16	90.00 ± 0.33	200.54 ± 0.36	**35.34 ± 0.42**	230.37 ± 0.65	137.13 ± 0.44
	115	4400.00 ± 1.05	70.47 ± 0.15	165.00 ± 0.05	34.18 ± 0.33	210.21 ± 0.15	110.25 ± 0.15
	121	4200.54 ± 0.51	43.00 ± 0.05	80.00 ± 0.34	33.14 ± 0.22	185.17 ± 0.53	92.78 ± 0.05
pH		4760.52 ± 0.13	210.00 ± 0.32	405.00 ± 0.15	10.12 ± 0.17	65.44 ± 0.11	14.35 ± 0.03
	3	4690.00 ± 0.23	185.00 ± 1.05	390.00 ± 0.17	13.42 ± 0.03	76.26 ± 0.02	20.25 ± 0.15
	4	4645.05 ± 0.31	155.00 ± 0.02	375.50 ± 0.10	23.45 ± 0.05	85.55 ± 0.15	36.50 ± 0.22
	5	4550.00 ± 0.53	135.00 ± 1.00	335.00 ± 0.22	21.16 ± 0.13	82.32 ± 0.23	44.31 ± 0.10
	6	4500.00 ± 0.50	110.50 ± 0.05	315.06 ± 0.17	14.45 ± 0.11	140.24 ± 0.13	74.54 ± 0.08
	7	4500.00 ± 0.42	107.00 ± 0.06	312.00 ± 0.13	12.34 ± 0.05	170.47 ± 0.08	106.45 ± 0.05
	8	4500.00 ± 0.40	105.45 ± 0.50	310.00 ± 0.11	7.18 ± 0.12	170.33 ± 0.06	88.183 ± 0.01
	9	4500.00 ± 0.41	105.00 ± 0.23	310.00 ± 0.03	5.56 ± 0.04	90.61 ± 0.11	39.76 ± 0.15
	10	4500.00 ± 0.05	105.00 ± 0.50	300.30 ± 0.14	–	71.45 ± 0.05	15.08 ± 0.07
	11	4185.67 ± 0.11	95.00 ± 0.41	285.00 ± 0.04	–	38.33 ± 0.22	6.36 ± 0.11
	12	3300.56 ± 0.23	75.55 ± 0.15	190.54 ± 0.10	–	–	–
Cations [0.1–3%]	NaCl	2254.55 ± 0.07	88.00 ± 0.05	275.00 ± 0.12	–	175.45 ± 0.13	29.33 ± 0.05
	KCl	2150.00 ± 0.25	75.00 ± 0.11	225.00 ± 0.05	–	180.33 ± 0.15	25.75 ± 0.13
	MgCl$_2$	4600.00 ± 0.33	170.40 ± 0.05	380.00 ± 0.22	40.48 ± 0.18	385.45 ± 0.01	115.55 ± 0.15
	CaCl$_2$	4680.00 ± 0.23	205.43 ± 0.22	425.54 ± 0.05	41.55 ± 0.14	400.23 ± 0.32	125.00 ± 0.14
	FeCl$_3$	4692.00 ± 0.12	220.00 ± 0.32	435.00 ± 0.14	**42.81 ± 0.06**	NT	NT
	Al$_2$(SO$_4$)$_3$	4697.00 ± 0.15	230.00 ± 0.03	490.25 ± 0.21	41.23 ± 0.05	NT	NT

NT – not tested, (–) – no gelling

sence of G-blocks, high M/G ratio, alternating MG/GM (mixed sequences), high DP_n (172), and acetylated M-residues. The high Mol. wt, equal distribution of alternating MG/GM-blocks (12%) and MGM-blocks (12%), the water-binding capacity of O-acetyl groups, and some limited binding specificity towards divalent cations may also contribute to this observation (Geddie and Sutherland, 1994; Drage and Taylor, 2011). These findings suggest that CMG1418 alginate can serve as an alternative soft and elastic gelling and thickening agent in textile printing, papermaking, pharmaceuticals, beverages, dairy products, and food formulations, to improve quality attributes and enhance the shelf-life and restructuration of fruits and vegetables, fish, and meat (Valentine et al., 2020).

Viscosity of CMG1418 alginate

The viscosities demonstrated by CMG1418 alginate were found to be stable at temperatures ranging from 20 to 100°C. However, as the temperature increased beyond 100°C or decreased below 20°C, the viscosities gradually decreased at a rate of about 0.45 and 0.44%/°C, respectively (Table 5). These results indicated the thermostable rheological behavior of CMG1418 alginate at temperatures between 20 and 100°C, thus highlighting the thermal strength of the polymer's core backbone. Additionally, the viscosity of CMG1418 alginate was observed to increase (1.5%/°C) at a pH < 6 and remained unaffected between pH 6 and 9. However, it decreased at pH > 10 (Table 5). The increase in viscosity at pH < 6 might be attributed to the protonation of free COO^- ions present in the polymeric chain to –COOH, which reduces the electrostatic repulsion between adjacent chains, bringing them closer to each other to form stronger hydrogen bonds, thus exhibiting higher viscosities (King, 1983). On the other hand, at pH > 10, a slow depolymerization process might occur, resulting in a fall in viscosity (Qin, 2018).

The addition of monovalent NaCl and KCl cations (0.1–5%) resulted in reduced viscosity (Table 5). Alginate dissolved in the solution is reported to exhibit polyelectrolyte behavior and high viscosity due to the negative charges on carboxylic groups. However, the addition of monovalent cation salts to the solution can reduce viscosity by lowering the electric charges between molecular chains and reducing chain extension (Qin, 2018). As a result, entanglement between molecular chains is

reduced, leading to a drop-in solution viscosity upon the addition of monovalent salt (Qin, 2018). Conversely, the addition of 0.1–5% divalent ($CaCl_2$, $MgCl_2$) and multivalent {$FeCl_3$, $Al_2(SO_4)_3$} cations resulted in slightly increased viscosity compared to salt-free solution. Divalent and multivalent cations are believed to bind solely to G-blocks to form a more viscous hydrogel by ionic cross-linking (Lee and Mooney, 2012). In the present study, due to the presence of high MM, high M/G ratio, and absence of poly-G-blocks in CMG1418 alginate, divalent and multivalent cations could not establish crosslinking ionic interactions except with G residues of alternating MG/GM-block, thus forming a more viscous hydrogel (Lee and Mooney, 2012).

These results indicate that the viscosity of CMG1418 alginate measured under various conditions was higher and promising, as it significantly surpassed that of commercial sodium alginate SG-500 and FD-120 over a broad range of temperatures and pH (Table 5). Alginate rheological behavior has been linked to high polymeric chain length (Mol. wt) (Senuma et al., 2000), epimerization of G-residues, and higher DOA of M-residues, which diminishes the affinity of alginate for cations. These properties are present in CMG1418 alginate (Skjåk-Bræk et al., 1989; Storz et al., 2009). Based on viscosity, alginates have been classified into three categories: low viscosity alginate (< 240 mPas), medium viscosity alginate (240–3500 mPas), and high viscosity alginate (> 3500 mPas) (Rasyid, 2003). Thus, according to this classification, CMG1418 alginate could be classified as high viscosity alginate.

In summary, the unique structural composition of CMG1418 alginate, which includes a distribution of mostly poly-M blocks without poly-G blocks, a high M/G ratio, and O-acetyl groups at O-2 and/or O-3 exclusively on M-residues, along with its DP_n (Mol. wt), is responsible for its exceptional material and functional properties. These properties are not found in alginates from algae, *Azotobacter*, or other *Pseudomonas* species, and cannot be replicated by synthetic chemistry. As such, this study represents the first investigation of the distinctive functional properties of a physiochemically consistent bacterial alginate. The results demonstrate that CMG1418 alginate offers highly promising and significant gelling, stabilizing, thickening, flocculating, and water absorption and retention properties, surpas-

sing those of algal alginates, and can be utilized across a wide range of applications in food and nonfood industries, as well as in biomedical and bioengineering fields.

Conclusion

In conclusion, this study has contributed to a better understanding of biosynthesis, structure–physical properties relationship, and the importance of structurally consistent bacterial alginate for potential applications. The unique and structurally consistent CMG1418 alginate demonstrated significantly higher and consistent viscosifying, soft gelling, flocculating, water-holding, and emulsifying properties over a broad range of pH and temperatures when compared to currently used algal alginates. These findings suggest that CMG1418 alginate could be a promising and reliable alternative to inconsistent algal alginates, particularly in applications that require thickening, soft gelling, viscosifying, flocculating, emulsifying, and water absorption properties.

References

Abraham A., Afewerki B., Tsegay B., Ghebremedhin H., Teklehaimanot B., Reddy K.S. (2018) *Extraction of agar and alginate from marine seaweeds in red sea region*. Int. J. Mar. Biol. Res. (2): 1–8. https://doi.org/10.15226/24754706/3/2/00126

Anastassiou E.D., Mintzas A.C., Kounavis C., Dimitracopoulos G. (1987) *Alginate production by clinical nonmucoid Pseudomonas aeruginosa strains*. J. Clin. Microbiol. 25(4): 656–659. https://doi.org/10.1128/jcm.25.4.656-659.1987

Arunkumar K. (2017) *Extraction, isolation, and characterization of alginate*. [in:] *Industrial applications of marine biopolymers*. Ed. Sudha P.N., Boca Raton, Florida: CRC Press: 21–37. https://doi.org/10.4324/9781315313535

Bai S., Chen H., Zhu L., Liu W., Yu H.D., Wang X., Yin Y. (2017) *Comparative study on the in vitro effects of Pseudomonas aeruginosa and seaweed alginates on human gut microbiota*. PLoS One 12(2): e0171576. https://doi.org/10.1371/journal.pone.0171576H

Bjerkan T.M., Lillehov B.E., Strand W.I., Skjåk-Bræk G., Valla S., Ertesvåg H. (2004a) *Construction and analyses of hybrid Azotobacter vinelandii mannuronan C-5 epimerases with new epimerization pattern characteristics*. Biochem. J. 381: 813–821. https://doi.org/10.1042/BJ20031580

Bjerkan T.M., Bender C.L., Ertesvåg H., Drabløs F., Fakhr M.K., Preston L.A., Skjåk-Bræk G., Valla S. (2004b) *The Pseudomonas syringae genome encodes a combined mannuronan C-5 epimerase and O-acetylhydrolase, which strongly enhances the predicted gel-forming properties of alginates*. J. Biol. Chem. 279: 28920–28929. https://doi.org/10.1074/jbc.M313293200

Brzezińska M., Szparaga G. (2015) *The effect of sodium alginate concentration on the rheological parameters of spinning solutions*. Autex Res. J. 15(2): 123–126. https://doi.org/10.2478/aut-2014-0044

Carlson D.M., Matthews L.W. (1966) *Polyuronic acids produced by Pseudomonas aeruginosa*. Biochemistry 5: 2817–2822.

Drage K., Taylor C. (2011) *Chemical, physical and biological properties of alginates and their biomedical implications*. Food Hydrocoll. 25(2): 251–256. https://doi.org/10.1016/j.foodhyd.2009.10.007

Dudun A.A., Akoulina E.A., Zhuikov V.A., Makhina T.K., Voinova V.V., Belishev N.V., Khaydapova D.D., Shaitan K.V., Bonartseva G.A., Bonartsev A.P. (2022) *Competitive biosynthesis of bacterial alginate using Azotobacter vinelandii 12 for tissue engineering applications*. Polymers 14: 131. https://doi.org/10.3390/polym14010131

Eremwanarue O.A., Nwawuba S.U., Shittu O.H. (2021) *Characterization of the prevailing multidrug Pseudomonas aeruginosa strains from surgical wound using 16S rRNA sequencing technique*. Malays. J. Med. Sci. 28(4): 37–49. https://doi.org/10.21315/mjms2021.28.4.5

Ertesvåg H. (2015) *Alginate-modifying enzymes: biological roles and biotechnological uses*. Front. Microbiol. 6(523): 2–8. https://doi.org/10.3389/fmicb.2015.00523

Fertah M., Belfkira A., Dahmane E., Taourirte M., Brouillette F. (2017) *Extraction and characterization of sodium alginate from moroccan laminaria digitata brown seaweed*. Arab. J. Chem. 10: 3707–3714. https://doi.org/10.1016/j.arabjc.2014.05.003

Fialho A.M., Zielinski N.A., Fett W.F., Chakrabarty A.M., Berry A. (1990) *Distribution of alginate gene sequences in the Pseudomonas ribosomal RNA homology group I-Azomonas-Azotobacter lineage of superfamily B prokaryotes*. Appl. Environ. Microbiol. 56: 436–443. https://doi.org/10.1128/aem.56.2.436-443.1990

Flores C., Díaz-Barrera A., Martínez F., Galindo E., Peña C. (2015) *Role of oxygen in polymerisation and depolymerization of alginate produced by Azotobacter vinelandii*. J. Chem. Technol. Biotechnol. 90: 356–365. https://doi.org/10.1002/jctb.4548

Franklin M.J., Ohman D.E. (1996) *Identification of algI and algJ in Pseudomonas aeruginosa alginate biosynthetic gene cluster which are required for alginate O-acetylation*. J. Bacteriol. 178(8): 2186–2195. https://doi.org/10.1128/jb.178.8.2186-2195.1996

Franklin M.J., Ohman D.E. (2002) *Mutant analysis and cellular localization of the AlgI, algJ, and AlgF proteins required for O-acetylation alginate in Pseudomonas aeruginosa*. J. Bacteriol. 184(11): 3000–3007. https://doi.org/10.1128%2FJB.184.11.3000-3007.2002

Fyfe J.A.M., Govan J.R.W. (1983) *Synthesis, regulation and biological function of bacterial alginate*. Prog. Ind. Microbiol. 18: 45–83. https://doi.org/10.1128/ AEM.66.9.4037-4044.2000

Geddie J.L., Sutherland I.W. (1994) *The effect of acetylation on cation binding by algal and bacterial alginates*. Biotechnol. Appl. Biochem. 20: 117–129.

Goh C.H., Heng P.W.S., Chen L.W. (2012) *Alginates as a useful natural polymer for microencapsulation and therapeutic applications.* Carbohydr. Polym. 88: 1–12. https://doi.org/10.1016/j.carbpol.2011.11.012

Grasdalen H. (1983) *High-field, ¹H-NMR spectroscopy of alginate sequential structure and linkage conformations.* Carbohydr. Res. 118: 255–260. https://doi.org/10.1016/0008-6215(83)88053-7

Hills O.J., Smith J., Scott A.J., Devine D.A., Chappell H.F. (2021) *Cation complexation by mucoid Pseudomonas aeruginosa extracellular polysaccharide.* PLoS One. 16(9): e0257026. https://doi.org/10.1371/journal.pone.0257026

Kam N., Park Y.J., Kim H.S. (2011) *Molecular identification of a polyM-specific alginate lyase from Pseudomonas sp. strain KS-408 for degradation of glycosidic linkages between two mannuronates or mannuronate and guluronate in alginate.* Can J. Microbiol. 57: 1032–1041. https://doi.org/10.1139/w11-106

King A.H. (1983) *Brown seaweed extracts (alginates).* [in:] *Food hydrocolloids.* Ed. Glicksman M., Boca Raton, Florida: CRC Press: 115–188.

Koti B.A., Manohar S., Lalitha J. (2014) *Media optimization for depolymerization of alginate by Pseudomonas aeruginosa AG LSL-11.* Int. Lett. Nat. Sci. 14: 30–39. https://doi.org/10.18052/www.scipress.com/ILNS.19.30

Kurane R., Nohata Y. (1991) *Microbial flocculation of waste liquids and oil emulsion by a bioflocculant from Alcaligenes latus.* Agric. Biol. Chem. 55(4): 1127–1129. https://doi.org/10.1080/00021369.1991.10870738

Kurane R., Nohata Y. (1994) *A new water-absorbing polysaccharide from Alcaligenes latus.* Biosci. Biotech. Biochem. 58(2): 235–238. https://doi.org/10.1271/bbb.58.235

Lee K.Y., Mooney D.J. (2012) *Alginate: properties and biomedical applications.* Prog. Polym. Sci. 37(1): 106–126. https://doi.org/10.1016/j.progpolymsci.2011.06.003

Leitào J.H., Fialho A.M., Sa-Corre I. (1992) *Effects of growth temperature on alginate synthesis and enzymes in Pseudomonas aeruginosa variants.* J. Gen. Microbiol. 138: 605–610. https://doi.org/10.1099/00221287-138-3-605

MacDowell R.H. (1974) *Properties of alginates.* 3rd ed. London: Alginate Industries Limited.

Madilyn F., Floodgate G.D. (1973) *An electron-microscopic demonstration of an acidic polysaccharide involved in the adhesion of a marine bacterium to a solid surface.* J. Gen. Microbiol. 74: 325–334.

Mancini M., Moresi M., Rancini R. (1999) *Mechanical properties of alginate gels: empirical characterization.* J. Food Eng. 39(4): 369–378. https://doi.org/10.1016/S0260-8774(99)00022-9

Manresa A., Spuny M.J., Guinia J., Comelles F. (1987) *Characterization and production of a new extracellular polymer from Pseudomonas GSP-910.* Appl. Microbiol. Biotechnol. 26: 347–351.

Marinho-Soriano E., Fonseca P.C., Carneiro M.A., Moreira W.S. (2006) *Seasonal variation in the chemical composition of two tropical seaweeds.* Biores. Technol. 97: 2402–2406. https://doi.org/10.1016/j.biortech.2005.10. 014

Meena S., Vidya K.M., Tripathic A.D., Ts R.L. (2020) *Optimization and characterization of alginic acid synthesized from a novel strain of Pseudomonas stutzeri.* Biotechnol. Rep. 27: e00517. https://doi.org/10.1016/j.btre.2020.e00517.

Michaels A.S. (1954) *Aggregation of suspensions by polyelectrolytes.* Ind. Eng. Chem. 46: 1485–1490. https://doi.org/10.1021/ie50535a049

Moradali M.F., Donati I., Sims I.M., Ghods S., Rehm B.H.A. (2015) *Alginate polymerization and modification are linked in Pseudomonas aeruginosa.* mBio 6(3): e00453-415. https://doi.org/10.1128/mBio.00453-15

Moscovici M. (2015) *Present and future medical applications of microbial exopolysaccharides.* Front. Microbiol. 6: 1012. https://doi.org/10.3389/fmicb.2015.01012

Mosmann T.T. (1983) *Rapid colorimetric assay for cellular growth and survival: application to proliferation and cytotoxicity assays.* J. Immunol. Methods. 65: 55–63.

Muhammadi, Ahmed N. (2006) *Phenotypic diversity among indigenous soil bacterial strains from different geographical regions of Karachi.* Int. J. Biol. Biotechnol. 3(4): 733–738.

Muhammadi, Shafiq S. (2019) *Genetic, structural and pharmacological characterization of polymannuronate synthesized by algG mutant indigenous soil bacterium Pseudomonas aeruginosa CMG1421.* J. Appl. Microbiol. 126(1): 113–126. https://doi.org/10.1111/jam.14098

Narbad A., Hewlins M.J.E., Gacesa P., Russell N.J. (1990) *The use of ¹³C-n.m.r. spectroscopy to monitor alginate biosynthesis in mucoid Pseudomonas aeruginosa.* Biochem. J. 267: 579–584. https://doi.org/10.1042%2Fbj2670579

Nivens D.E., Ohman D.E., Williams J., Franklin M.J. (2001) *Role of alginate and its O-acetylation in the formation of Pseudomonas aeruginosa microcolonies and biofilm.* J. Bacteriol. 183(3): 1047–1057. https://doi.org/10.1128/JB.183.3.1047-1057.2001

Ogle J.W., Janda J.M., Woods D.E., Vasil M.L. (1987) *Characterization and use of a DNA probe as an epidemiological marker for Pseudomonas aeruginosa.* J. Infect. Dis.155: 119–126. https://doi.org/10.1093/infdis/155.1.119

Qin Y. (2018) *Bioactive seaweeds for food applications.* London: Academic Press Elsevier.

Rasyid A. (2003) *Algae coklat (Phaeophyta) sebagai sumber alginate.* Oseana 28(1): 33–38.

Remminghorst U., Rehm B.H.A. (2006) *Bacterial alginates: from biosynthesis to applications.* Biotechnol. Lett. 28(21): 1701–1712. https://doi.org/10.1007/s10529-006-9156-x

Ruehrwein R.A., Ward D.W. (1952) *Mechanism of clay aggregation by polyelectrolytes.* Soil Sci. 73: 485–492.

Sabra W., Zeng A.P., Lunsdorf H., Deckwer W.D. (2000) *Effect of oxygen on formation and structure of Azotobacter vinelandii alginate and its role in protecting nitrogenase.* Appl. Environ. Microbiol. 66(9): 4037–4044. https://doi.org/10.1128/aem.66.9.4037-4044.2000

Sachan K.N., Pushkar S., Jha A., Bhattcharya A. (2009) *Sodium alginate: the wonder polymer for controlled drug delivery.* J. Pharm. Res. 2(8): 1191–1199.

Schürks N., Wingender J., Flemming H.C., Mayer C. (2002) *Monomer composition and sequence of alginates from Pseudomonas aeruginosa*. Int. J. Biol. Macromol. 30: 105–111. https://doi.org/10.1016/S0141-8130(02)00002-F8

Senuma Y., Lowe C., Zweifel Y., Hilborn J.G., Marison I. (2000) *Alginate hydrogel microspheres and microcapsules prepared by spinning disk atomization*. Biotechnol. Bioeng. 67(5): 616–622. https://doi.org/10.1002/(SICI) 1097-0290(20000305)67:5<616::AID-BIT12>3.0.CO;2-Z

Skjåk-Bræk G., Grasdalen H.B., Larsen B. (1986) *Monomer sequence and acetylation pattern in some bacterial alginates*. Carbohydr. Res. 154: 239–250. https://doi.org/10.1016/S0008-6215(00)90036-3

Skjåk-Bræk G., Zanetti F., Paoletti S. (1989) *Effect of acetylation on some solution and gelling properties of alginate*. Carbohydr. Res. 185: 131–138. https://doi.org/10.1016/0008-6215(89)84028-5

Stewart M.B., Myat D.T., Kuiper M., Manning R.J., Gray S.R., Orbell J.D. (2017) *A structural basis for the amphiphilic character of alginates-implications for membrane fouling*. Carbohydr. Polym. 164: 162–169. https://doi.org/10.1016/j.carbpol.2017.01.072

Storz H., Zimmermann U., Zimmermann H., Kulicke W-M. (2009) *Viscoelastic properties of ultra-high viscosity alginates*. Rheol. Acta. 49(2): 155–167. https://doi.org/10.1007/s00397-009-0400-x

Sutherland I.W. (1990) *Biotechnology of microbial exopolysaccharides*. Cambridge: Cambridge University Press. https://doi.org/10.1017/CBO9780511525384

Tawila Z.M.A., Ismail S., Dadrasnia A., Usman M.M. (2018) *Production and characterization of a bioflocculant produced by Bacillus salmalaya 139SI-7 and its applications in wastewater treatment*. Molecules 23(10): 2689. https://doi.org/10.3390/molecules23102689

Urtuvia V., Maturana N., Acevedo F., Peña C., Diaz Barrera A. (2017) *Bacterial alginate production: an overview of its biosynthesis and potential industrial production*. World J. Microbiol. Biotechnol. 33: 198. https://doi.org/10.1007/s11274-017-2363-x

Usov A.I. (1999) *Alginic acid and alginate: analytical methods used for their estimation and characterization of composition and primary structure*. Russ. Chem. Rev. 68(11): 957–966. https://doi.org/10.1070/RC1999v068n11ABEH 000532

Valentine M.E., Kirby B.D., Withers T.R., Johnson S.L., Long T.E., Hao Y., Lam J.S., Niles R.M., Yu H.D. (2020) *Generation of a highly attenuated strain of Pseudomonas aeruginosa for commercial production of alginate*. Microb. Biotechnol. 13(1): 162–175. https://doi.org/10.1111/1751-7915.13411

Windhues T., Borchard W. (2003) *Effect of acetylation on physico-chemical properties of bacterial and algal alginates in physiological sodium chloride solutions investigated with light scattering techniques*. Carbohydr. Polym. 52: 47–52. https://doi.org/10.1016/S0144-8617(02)00265-5

Yalpani M., Sandford P.A. (1987) *Commercial polysaccharides: recent trends and developments*. [in:] *Industrial polysaccharides*. Ed. Yalpani M., Amsterdam: Elsevier Sci. Publ.: 311–335.

Zhang J., Cheng Q.A. (2021) *Preparation of alginate-based biomaterials and their applications in biomedicine*. Mar. Drugs. 19(5): 264. https://doi.org/10.3390/md 19050264